

Table 1 Clinical characteristics.

Patient no.	Gender	Onset age (months)	Age at surgery (months)	Seizure frequency	Seizure type at surgery	Spasm history	Localization of FCD	Interictal EEG discharge	AEDs at surgery	Histo-pathology	Follow-up (years)	Seizure outcome
1	Girl	5	18	Daily	CPS		R-frontal lobe	Regional	PHT, PB, ZNS	IA	5	I
2	Girl	4	54	Daily	CPS		L-frontal lobe	Localized	VPA, CBZ, PHT	II B	3	I
3	Boy	17	84	Daily	CPS		R-multiple lobes (parieto-temporo-occipital)	Localized	CBZ	II A	7	I
4	Girl	7	92	Daily	CPS		R-frontal lobe	widespread	CBZ	II B	3	I
5	Girl	12	49	Daily	spasm		R-frontal lobe	Regional	VPA, PHT	IB	2	I
6	Boy	0.7	59	Daily	CPS	+	R-multiple lobes (temporo-occipital)	Regional	VPA, PHT	II B	2	I
7	Boy	24	62	Daily	CPS		R-frontal lobe	Localized	PHT	II B	2	I
8	Boy	16	52	Daily	CPS		L-multiple lobes (fronto-temporal)	Localized	CBZ	II B	2	I
9	Boy	26	64	Daily	CPS		R-frontal lobe	Regional	CBZ, ZNS	II A	2	I
10	Boy	36	96	Daily	CPS		R-frontal lobe	Localized	CBZ, PHT, CLB	II B	3	I
11	Girl	0.5	101	Daily	CPS		L-frontal lobe	Localized	VPA, ZNS	II B	8	II
12	Girl	8	80	Daily	CPS		R-frontal lobe	Localized	CBZ, PHT	II B	2	II
13	Girl	1	112	Daily	CPS		L-multiple lobes (temporo-occipital)	Localized	VPA, CBZ, PHT, CLB	II B	2	III
14	Girl	1	46	Daily	CPS	+	R-multiple lobes (temporo-occipital)	Regional	VPA, ZNS	II A	3	III
15	Boy	7	45	Daily	CPS		L-frontal lobe	Localized	VPA, PHT	IB	2	III
16	Boy	15	145	Daily	CPS		R-frontal lobe	Localized	CBZ, PB	II B	2	III
17	Boy	14	118	Daily	CPS		R-frontal lobe	Regional	VPA, CBZ, PHT, AZA	II B	5	IV
Mean ± SD		11.4 ± 10.1	75.1 ± 32.4								3.2 ± 1.9	
Median		8.0	64.0								2	

CPS: complex partial seizure, R: right, L: left, FCD: focal cortical dysplasia, EEG: electroencephalography, localized: epileptic discharges within FCD site, regional: epileptic discharges spread beyond FCD site, but within identified area, widespread: epileptic discharges not confined to specific area, AEDs: antiepileptic drugs, VPA: valproate, PHT: phenytoin, CBZ: carbamazepine, PB: phenobarbital, ZNS: zonisamide, CLB: clobazam, AZA: acetazolamide, R: right, L: left, EEG: electroencephalography, Seizure outcome: Engel's class.

Table 2 Presurgical and postsurgical developmental evaluations.

Patient no.	Group	Psychological test	Observation age		DQ-IQ			Mental age			RIMA (months/year)		
			Pre	Post	Pre	Post	Difference	Pre	Post	Difference	Pre	Post	Difference
1	1	MCC test	9m	6y6m	56	51*	-5	5m	3y4m	2y11m	6.7	6.1	-0.6
2	1	MCC test	3y	7y5m	28	35	7	1y3m	2y8m	1y5m	0.7	5.7	5.0
3	1	Tanaka scale	5y4m	12y	46	46	0	3y1m	5y6m	2y5m	1.9	5.2	3.3
4	1	Tanaka scale	4y6m	9y10m	64	71	7	4y6m	7y	2y6m	5.2	10.6	5.4
5	2	MCC test	2y	6y1m	33	34	-1	1y4m	2y1m	9m	5.0	4.3	-0.7
6	2	MCC test	3y7m	7y1m	16	14	-2	7m	1y	5m	-	1.4	-
7	3	Tanaka scale	4y8m	7y4m	74	84	10	3y6m	6y2m	2y8m	-	12.0	-
8	3	Tanaka scale	3y	6y7m	94	99	5	4y6m	6y6m	2y	-	12.3	-
9	3	Tanaka scale	3y1m	7y	79	81	2	3y9m	5y8m	1y11m	5.4	10.2	4.8
10	3	Tanaka scale	7y4m	10y10m	87	75	-12	6y5m	8y2m	1y9m	-	6.0	-
11	4	Tanaka scale	4y6m	14y6m	56	40	-16	3y8m	6y10m	3y1m	8.5	4.8	-3.7
12	4	Tanaka scale	5y5m	7y5m	45	27	-18	2y6m	2y	-6m	-	-3.0	-
13	4	MCC test	8y6m	11y6m	8	10	2	9m	11m	2m	-	1.7	-
14	4	MCC test	1y5m	7y	17	15	-2	7m	12m	5m	0.5	1.4	1.9
15	4	MCC test	3y6m	6y	33	35	2	1y 1m	2y	11m	-	5.1	-
16	4	Tanaka scale	11y6m	14y	41	42	1	4y 6m	6y	1y6m	-	7.2	-
17	4	Tanaka scale	8y6m	15y	22	15	-7	2y 2m	2y8m	6m	-	1.1	-

MCC test: Mother-Child Counseling baby test, Tanaka: Tanaka-Binet scale of intelligence, RIMA: Rate of mental age increase, pre: presurgical evaluation, post: the latest postsurgical evaluation, DQ/IQ: developmental quotient or intelligence quotient.

* Examination by Tanaka-Binet scale of intelligence, y: year, m: month.

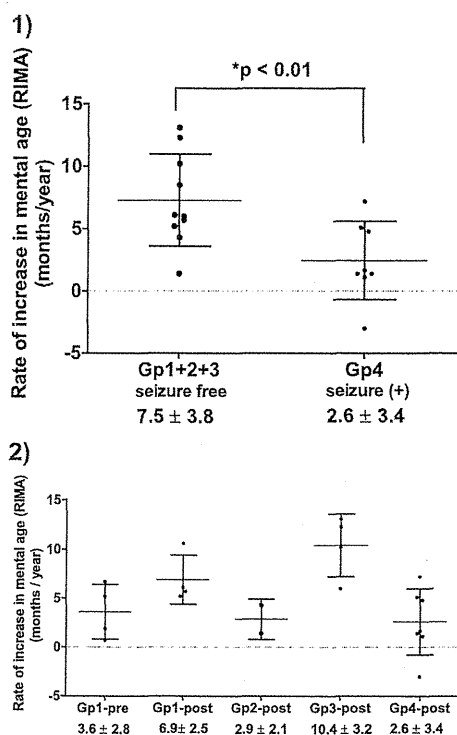


Fig. 3 (1) Comparison of rate of increase in mental age between seizure-free and seizure (+) groups. Gp: Group, * significant difference between group 1 + 2 + 3 and group 4 (unpaired *t* test with Welch's correction, $t = 2.99$, $df = 15$, $p = 0.0092$); Data were analyzed using GraphPad Prism 5 (GraphPad Software Inc., San Diego, CA, USA). (2) Rate of increase in mental age in four groups. Gp: Group, pre: presurgical evaluation, post: postsurgical evaluation. Data were calculated using GraphPad Prism 5 (GraphPad Software Inc., San Diego, CA, USA).

increases in mental age, 14 had RIMA lower than the normal average of 12 months/year, and the remaining 2 (Patients 7 and 8) had RIMA around 12 months/year (Table 2).

RIMA after surgery was significantly greater in ten patients with seizure control (groups 1–3; 7.5 ± 3.8 months/year) than in seven patients without seizure control (group 4; 2.6 ± 3.4 months/year) (unpaired *t*-test with Welch's correction, $t = 2.99$, $df = 15$, $p = 0.0092$) (Fig. 3 - 1). Among patients with seizure control, mean RIMA in those with spasm (group 2) was 2.9 ± 2.1 months/year, but mean RIMA in patients without spasm (groups 1 and 3) was 8.5 ± 3.5 months/year. In group 1 (seizure control, $DQ-IQ < 70$ and no spasm), mean RIMA changed from 3.6 ± 2.8 months/year before surgery to 6.9 ± 2.5 months/year after surgery (Fig. 3 - 2). Postsurgical RIMA in group 1 was higher than that in group 4 (no seizure control).

Postsurgical RIMA in group 3 (seizure control and $DQ-IQ \geq 70$; 10.1 ± 2.9 months/year) was almost at a normal level (12 months/year), and was higher than that in group 2 (with spasm) and in group 4 (no seizure control). Of four patients with presurgical $DQ-IQ \geq 70$ and no spasm, two showed RIMA equal to or higher than normal average.

Group 1 is the category with partial seizures only (no spasms) and lower $IQ-DQ$ before surgery. Therefore, group

1 is the representative of most candidates for surgery. As patients of Group 1 achieved seizure control after surgery, their developmental evolution seems to be the best evidence for the benefit of surgery. The relations between mental age, chronological age and RIMA of 4 patients in group 1 are shown in Fig. 4. In Patient 1 who underwent surgery at the age of 1-year-6-month, postsurgical mental age increased from 7 months to 17 months between chronological ages 1-year-7-month and 3-year-5-month, and further increased from 17 months to 40 months between chronological ages 3-year-5-month and 6-year-6-month (Fig. 4). Accordingly, RIMA was elevated from 5.5 to 7.5 months/year, showing improvement after two years post-surgery. In patient 2, RIMA was 7.2 months/year between chronological ages 4-year-5-month and 4-year-10-month, and 6.0 months/year between chronological ages 6-year-5-month and 7-year-5-months. In patient 3, RIMA improved from 3.3 to 10.0 months/year after 2 years post-surgery. In patient 4, RIMA improved from 6.9 to 12.0 months/year after 1 month post-surgery.

Discussion

We studied the developmental outcome after surgery in 17 FCD patients with early-onset epilepsy at 3 years of age or younger. Ten patients (58.8%) became seizure-free, and 82.3% of patients had preserved or improved $DQ-IQ$. Previous studies reported that children did not show any significant change in IQ after epilepsy surgery (Jonas et al., 2005; Freitag and Tuxhorn, 2005). Our data suggest that in FCD patients with early-onset epilepsy, epilepsy surgery may be beneficial for seizure control and may preserve or improve cognitive development.

RIMA after surgery in ten patients with seizure control was higher than that in seven patients without seizure control. Patients with lower presurgical $DQ-IQ (< 70)$ and postsurgical Engel's class I showed improved RIMA after surgery. These results suggest that developmental outcome after surgery may be affected by seizure control after surgery. Developmental plasticity in young children is a manifestation of the healthy brain during the period of neuronal and synaptic elaboration (Shields, 2000; Klein et al., 2000). Frequent or continuous epileptic discharge may lead to elaboration of abnormal synaptic connections, resulting in inadequate recovery of development.

RIMA of two patients with spasm (group 2) were lower than those of eight patients in groups 1 and 3, although all these patients achieved seizure control. Among patients in group 4, patient 14 who had a history of spasm had relatively low RIMA (1.4) after surgery. These data suggest that pathology in the brain with spasm impairs development, even after the cessation of seizures. Therefore, developmental outcome after surgery may be affected by neuronal damage caused by preceding spasms. Further studies are needed to examine the relationship between postsurgical developmental outcome and spasms.

In four patients in group 1 (seizure control, presurgical $DQ-IQ < 70$), $DQ-IQ$ did not increase after surgery, but RIMA changed from 3.6 ± 2.8 before surgery to 6.9 ± 2.5 months/year after surgery. In group 1, RIMA started to improve after 2 years following surgery (Fig. 4). These data

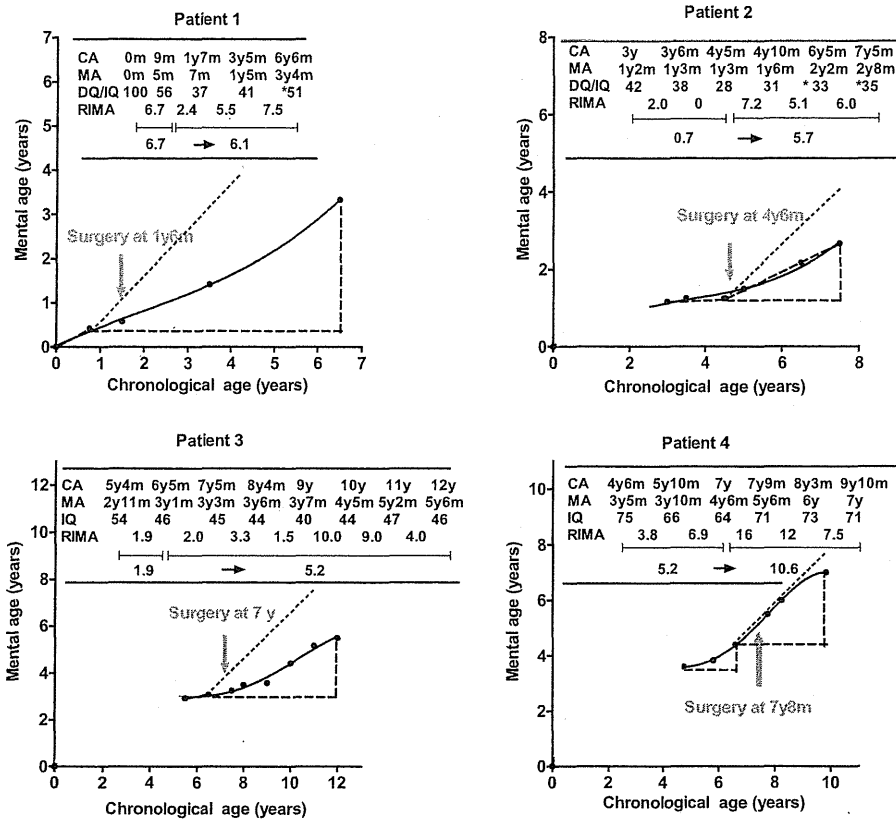


Fig. 4 Relations between mental age, chronological age and the rate of increase in mental age in 4 patients in group 1. Dotted lines show normal values. CA: chronological age, MA: mental age, IQ: intelligent quotient, RIMA: rate of increase in mental age (months/year) calculated as follows: mental age at the current evaluation – mental age at the last evaluation (months)/chronological interval between two evaluations (year). Thus normal average of RIMA is 12 months/year, y: years, m: months. * Presurgical test was examined by Mother-Child Counseling baby test and postsurgical test was examined by Tanaka-Binet scale of intelligence.

suggest that a catch-up of development needs a certain period for biological repair and maturation of the brain after cessation of seizure-related brain damage.

All data of postsurgical RIMA in group 1 were lower than normal average (12 months/year). In group 3, two of four patients showed RIMA increase equal to or higher than normal average. These results suggest that lower DQ-IQ before surgery is a risk factor for poor development after surgery. Previous study has also reported that presurgical cognitive level is the only factor independently associated with postsurgical IQ (Argenzio et al., 2011). Further long-term studies are required to reveal the factors affecting development after surgery. As FCD patients with early-onset epilepsy usually have refractory disabling seizures and impairment of cognition, we recommend early epilepsy surgery, especially when there is no history of spasm and definitive focus confirmed by presurgical evaluation.

Due to the limitation of the retrospective study design, we cannot exclude the possibility that the antiepileptic drugs had adverse effects on cognitive development. In addition, the sample size was too small to conduct more detailed comparisons within groups. Further multi-center study is

required to examine a larger number of patients with FCD who undergo surgery for early-onset epilepsy during earlier periods of the disease, and analyze the effectiveness of epilepsy surgery for development. Another limitation of this study was the indirect computation of intelligence and development measures.

Conclusions

In 58.8% of FCD patients with early-onset epilepsy, epilepsy surgery effectively controlled seizures, and in 82.3% of the patients, epilepsy surgery preserved or improved development. Residual seizures after surgery and lower DQ-IQ before surgery were identified as potential risk factors for poor development after surgery. In patients with seizure control and lower presurgical DQ-IQ, catch-up increase in mental age was observed after two years following surgery.

Acknowledgements

We thank Dr. Tadahiro Mihara who performed the surgeries from 1985, and the neuropsychologists at the National

Epilepsy Center, Shizuoka. We would like to express our gratitude to the patients and their families for their cooperation. This work was supported by Grants-in-aid for Scientific Research I Nos. 21591342, 23591238 and 24591537 (Y.T.); Comprehensive Research on Disability Health and Welfare; Research on Rare and Intractable Diseases (Y.T.) and grants from The Japan Epilepsy Research Foundation (Y.T.).

References

- Argenzio, L.D., Colonnelli, M.C., Harrison, S., Jacques, T.S., Harkness, W., Vargha-Khadem, F., Scott, R.C., Cross, J.H., 2011. Cognitive outcome after extratemporal epilepsy surgery in childhood. *Epilepsia* 52 (11), 1966–1972.
- Engel Jr., J., Van Ness, P.C., Rasmussen, T.B., Ojemann, L.M., 1993. Outcome with respect to epileptic seizures. In: Engel Jr., J. (Ed.), *Surgical Treatment of the Epilepsies*, second ed. Raven Press, New York, NY, pp. 609–621.
- Fauser, S., Huppertz, H.J., Bast, T., Strobl, K., Pantazis, G., Altenmueller, D.M., Feil, B., Rona, S., Kurth, C., Rating, D., Korinthenberg, R., Steinhoff, B.J., Volk, B., Schulze-Bonhage, A., 2006. Clinical characteristics in focal cortical dysplasia: a retrospective evaluation in a series of 120 patients. *Brain* 129, 1907–1916.
- Freitag, H., Tuxhorn, I., 2005. Cognitive function in preschool children after epilepsy surgery: rationale for early intervention. *Epilepsia* 46 (4), 561–567.
- Jonas, R., Asarnow, R.F., LoPresti, C., Yudovin, S., Koh, S., Wu, J.Y., Sankar, R., Shields, W.D., Vinters, H.V., Mathern, G.W., 2005. Surgery for symptomatic infant-onset epileptic encephalopathy with and without infantile spasms. *Neurology* 64 (4), 746–750 (22).
- Klein, B., Levin, B.E., Duchowny, M.S., Llabre, M.M., 2000. Cognitive outcome of children with epilepsy and malformations of cortical development. *Neurology* 55 (2), 230–235 (25).
- Koga, Y., 1967. *Mother–Child–Counseling Baby Test*. Doubun Shoin, Tokyo (in Japanese).
- Krsek, P., Pieper, T., Karlmeier, A., Hildebrandt, M., Kolodziejczyk, D., Winkler, P., Pauli, E., Blümcke, I., Holthausen, H., 2009. Different presurgical characteristics and seizure outcomes in children with focal cortical dysplasia type I or II. *Epilepsia* 50 (1), 125–137.
- Kuzniecky, R., Murro, A., King, D., Morawetz, R., Smith, J., Powers, R., Yaghai, F., Faught, E., Gallagher, B., Snead, O.C., 1993. Magnetic resonance imaging in childhood intractable partial epilepsies: pathologic correlations. *Neurology* 3 (4), 681–687.
- Loddenkemper, T., Holland, K.D., Stanford, L.D., Kotagal, P., Bingaman, W., Wyllie, E., 2007. Developmental outcome after epilepsy surgery in infancy. *Pediatrics* 119 (5), 930–935.
- Lortie, A., Plouin, P., Chiron, C., Delalande, O., Dulac, O., 2002. Characteristics of epilepsy in focal cortical dysplasia in infancy. *Epilepsy Res.* 51 (1–2), 133–145.
- Palmi, A., Najm, I., Avanzini, G., Babb, T., Guerrini, R., Foldvary-Schaefer, N., Jackson, G., Lüders, H.O., Prayson, R., Spreafico, R., Vinters, H.V., 2004. Terminology and classification of the cortical dysplasias. *Neurology* 62 (6 Suppl 3), S2–S8.
- Shields, W.D., 2000. Catastrophic epilepsy in childhood. *Epilepsia* 41 (Suppl 2), S2–S6.
- Sisodiya, S.M., Fauser, S., Cross, J.H., Thom, M., 2009. Focal cortical dysplasia type II: biological features and clinical perspectives. *Lancet Neurol.* 8 (9), 830–843.
- Tanaka, H., 1987. *Tanaka–Binet Scale of Intelligence*. Taken Shuppan, Tokyo (in Japanese).
- Tassi, L., Colombo, N., Garbelli, R., Francione, S., Lo Russo, G., Mai, R., Cardinale, F., Cossu, M., Ferrario, A., Galli, C., Brammerio, M., Citterio, A., Spreafico, R., 2002. Focal cortical dysplasia: neuropathological subtypes, EEG, neuroimaging and surgical outcome. *Brain* 125, 1719–1732.
- Taylor, D.C., Falconer, M.A., Bruton, C.J., Corsellis, J.A., 1971. Focal dysplasia of the cerebral cortex in epilepsy. *J. Neurol. Neurosurg. Psychiatry* 4 (4), 369–387.
- Widdess-Walsh, P., Kellinghaus, C., Jeha, L., Kotagal, P., Prayson, R., Bingaman, W., Najm, I.M., 2005. Electro-clinical and imaging characteristics of focal cortical dysplasia: correlation with pathological subtypes. *Epilepsy Res.* 67 (1–2), 25–33.
- Wyllie, E., 1996. Surgery for catastrophic localization-related epilepsy in infants. *Epilepsia* 37 (Suppl 1), S22–S25.

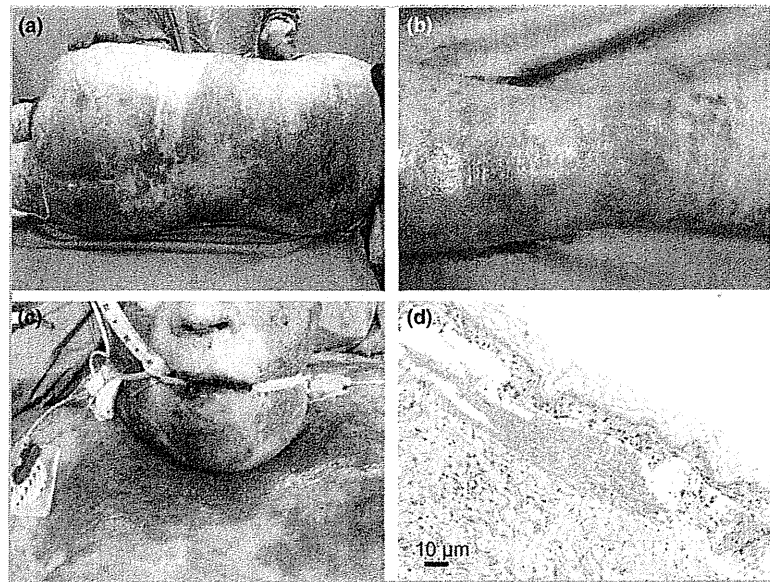


Fig 2. Photographs of skin manifestations in patient 2 following wound debridement, showing (a) the patient's back and (b) a lower leg with multiple macules, papules, blisters and erythematous and epidermolytic areas, typical of toxic epidermal necrolysis (TEN). (c) Involvement of the inner lip mucosa in this patient. (d) Haematoxylin and eosin-stained sections of a skin biopsy specimen of patient 2, with typical epidermolysis and leucocyte infiltrate of TEN.

taking herbal preparations in capsules, an imaginable common denominator of TEN development.

A single or multiplier effect by idiosyncratic, dose-related or drug-interactive reactions of phytochemicals or contaminants might be involved in the development of TEN in these patients. The objective evaluation by the Naranjo adverse drug reaction (ADR) probability scale⁹ calculated a possible ADR by the herbal remedy in cases 1 and 3 and a probable cause in case 2. In all cases, the TEN-specific algorithm for epidermal necrolysis (ALDEN) confirmed a possible cause of herbal remedies in TEN development.¹⁰

¹Department of Plastic, Hand and Reconstructive Surgery and ³Interdisciplinary Emergency and Disaster Medicine, Hannover Medical School, Hannover, Lower Saxony 30625, Germany

²Department of Plastic Surgery, Frenchay Hospital, Bristol, U.K.

E-mail: limbourg.anne@mh-hannover.de

A. LIMBOURG¹

A. STEIERT¹

A. JOKUSZKIS¹

K. YOUNG²

H.-A. ADAMS³

P.M. VOGT¹

5 Revuz J, Penso D, Roujeau JC et al. Toxic epidermal necrolysis. Clinical findings and prognosis factors in 87 patients. *Arch Dermatol* 1987; **123**:1160–5.

6 Araya OS, Ford EJ. An investigation of the type of photosensitization caused by the ingestion of St John's Wort (*Hypericum perforatum*) by calves. *J Comp Pathol* 1981; **91**:135–41.

7 Estrada JL, Gozalo F, Cecchini C, Casquete E. Contact urticaria from hops (*Humulus lupulus*) in a patient with previous urticaria-angioedema from peanut, chestnut and banana. *Contact Dermatitis* 2002; **46**:127.

8 Ernst E. Adverse effects of herbal drugs in dermatology. *Br J Dermatol* 2000; **143**:923–9.

9 Naranjo CA, Busto U, Sellers EM et al. A method for estimating the probability of adverse drug reactions. *Clin Pharmacol Ther* 1981; **30**:239–45.

10 Sassolas B, Haddad C, Mockenhaupt M et al. ALDEN, an algorithm for assessment of drug causality in Stevens-Johnson syndrome and toxic epidermal necrolysis: comparison with case-control analysis. *Clin Pharmacol Ther* 2010; **88**:60–8.

Funding sources: none.

Conflicts of interest: none declared.

References

- 1 Roujeau JC, Kelly JP, Naldi L et al. Medication use and the risk of Stevens-Johnson syndrome or toxic epidermal necrolysis. *N Engl J Med* 1995; **333**:1600–7.
- 2 Guillaume JC, Roujeau JC, Revuz J et al. The culprit drugs in 87 cases of toxic epidermal necrolysis (Lyell's syndrome). *Arch Dermatol* 1987; **123**:1166–70.
- 3 Goldstein LH, Elias M, Ron-Avraham G et al. Consumption of herbal remedies and dietary supplements amongst patients hospitalized in medical wards. *Br J Clin Pharmacol* 2007; **64**:373–80.
- 4 Newmaster SG, Ragupathy S, Dhivya S et al. Genomic valorization of the fine scale classification of small millet landraces in southern India. *Genome* 2013; **56**:123–7.

The serum level of HMGB1 (high mobility group box 1 protein) is preferentially high in drug-induced hypersensitivity syndrome/drug reaction with eosinophilia and systemic symptoms

DOI: 10.1111/bjd.13162

DEAR EDITOR, Drug-induced hypersensitivity syndrome (DIHS), also known as drug reaction with eosinophilia and systemic symptoms (DRESS), is characterized by high fever, multiple

organ involvement and haematological disorders, essentially without severe erythema or epidermal apoptosis.¹ Sequential reactivation of human herpes virus (HHV)-6 is deeply involved in the pathophysiology and persistence of DIHS/DRESS. A preceding increase in proinflammatory cytokines such as interleukin (IL)-6 and tumour necrosis factor (TNF)- α seems to be relevant to the viral reactivation in DIHS/DRESS, while the exact mechanism is still unclear.²

Stevens–Johnson syndrome (SJS) and toxic epidermal necrolysis (TEN), other severe cutaneous adverse drug reactions (cADRs), are characterized by high fever, severe erythema and widespread epidermal damage due to keratinocyte apoptosis. Activated cytotoxic T cells and natural killer cells are involved in SJS/TEN.³ The molecular cytotoxicity of Fas and cytotoxic proteins, including perforin/granzyme B and granulysin, are thought to contribute to induction of keratinocyte apoptosis.³ High mobility group box 1 protein (HMGB1) is a nonhistone nuclear protein that is released from severely damaged cells. HMGB1 plays a role in transcriptional regulation in the nucleus, while outside of the cell it serves as an activator of the inflammatory cascade.⁴ It was recently reported that HMGB1 levels are increased during the acute stage of SJS/TEN and can serve as an early diagnostic marker for SJS/TEN.⁵ However, the level of HMGB1 at the onset of other severe cADRs such as DIHS/DRESS has not been investigated. In addition, although there are limited reports on serum cytokine levels in cADRs,⁶ these cytokines have not been analysed with regards to HMGB1, which may induce aberrant cytokine production. To clarify the relationship between aberrant HMGB1 and cytokine production at disease onset, and the clinical manifestations elicited, we investigated serum HMGB1 and cytokine profiles in various cADRs.

Peripheral blood was taken from healthy controls and patients with various types of cADR including maculopapular (MP) type, erythema multiforme (EM), SJS, TEN and DIHS/DRESS at the time of onset and recovery. Onset is an acute exacerbation phase (< 7 days) and recovery is a remission phase of cADRs. Serum was stored at -80°C and cytokine levels were measured by lu-

minometric bead array using the Bio-Plex Suspension Array System (BioRad, Hemel Hempstead, U.K.). HMGB1 was measured by enzyme-linked immunosorbent assay. The groups consisted of the following subjects (full details in Table 1): healthy controls, 14 cases; MP/EM, 11 cases; SJS/TEN, 17 cases and DIHS/DRESS, 17 cases. For comparison of cytokine levels between healthy controls and each cADR group at onset, and between onset and recovery in each cADR group, the Mann–Whitney test and Wilcoxon matched-pairs tests were used, respectively. Statistical significance was established at $P < 0.05$ and $P < 0.01$.

HMGB1 was high in both SJS/TEN and DIHS/DRESS compared with healthy controls and other cADRs, but the level was significantly higher in DIHS/DRESS than in SJS/TEN. Comparison of cytokine levels between SJS/TEN and DIHS/DRESS revealed a prominent increase in T helper (Th)2 cytokines/chemokines such as IL-5, IL-9 and IL-13 in DIHS/DRESS. Additionally, IL-10 (an anti-inflammatory cytokine) and IL-12 were elevated in DIHS/DRESS (Fig. 1a). Concerning the serum cytokine levels at the time of onset in each group, the following were significantly increased compared with healthy controls: IL-5, IL-6, chemokine (C-X-C) motif ligand (CXCL)-8, IL-9, IL-12, eotaxin, granulocyte macrophage colony-stimulating factor (GM-CSF), CXCL-10 and vascular endothelial growth factor (VEGF) in MP/EM; IL-6, IL-12 and CXCL-10 in SJS/TEN; and IL-5, IL-6, IL-9, IL-10, IL-12, IL-13, IL-15, eotaxin, GM-CSF, interferon (IFN)- γ , CXCL-10 and VEGF in DIHS/DRESS. Proinflammatory cytokines such as TNF- α and IFN- γ were not necessarily high in severe cADRs. Most, but not all, cytokines returned to normal levels with treatment at the time of recovery (Fig. 1).

Although the levels of various types of serum cytokines were elevated at cADR onset, the levels of proinflammatory cytokines did not correlate with the types of cADR or disease severity. These results suggest that the overproduction of these cytokines contributes to promoting inflammation, but that mechanisms other than an increase of proinflammatory cytokines are essential for inducing the massive keratinocyte apoptosis observed in SJS/TEN.

In DIHS/DRESS, Th2 cytokines, HMGB1 and IL-10, were increased. Recent studies have reported that not only Th2 cytokines, but also Th2 chemokines such as thymus and activation-regulated chemokine, were elevated in serum in DIHS/DRESS.^{6,7} In addition, HMGB1 was more highly elevated than in SJS/TEN. HMGB1 has been shown to induce the differentiation of dendritic cells (DCs) to CD11c^{low}CD45RB^{high} DCs followed by shifting of Th1 to Th2 *in vitro*.⁸ Furthermore, high expression of HMGB1 in DIHS/DRESS skin has been reported.⁹ The area of expression of HMGB1 was larger in DIHS/DRESS lesions than in SJS lesions regardless of keratinocyte damage. Translocation of HMGB1 occurred in DIHS epidermal cells, and this HMGB1 attracted monomyeloid precursors harbouring HHV-6, resulting in HHV-6 transmission to skin-infiltrating CD4⁺ T cells, which is essential for HHV-6 replication in DIHS/DRESS. On the other hand, IL-10, which is an anti-inflammatory cytokine, was also highly elevated in DIHS/DRESS. It has been reported that expansion of Foxp3⁺CD25⁺ T regulatory cells (Tregs) was observed

Table 1 Profile of each group

Group	Number	Age (years), mean \pm SD	Sex, n (male/ female)	Type
Healthy controls	14	53.1 \pm 15.3	8/6	—
MP/EM	11	65.3 \pm 8.9	6/5	MP 6/EM 5
SJS/TEN	17	56.5 \pm 19.1	7/10	SJS 13/TEN 4
DIHS/DRESS	17	53.5 \pm 14.0	10/7	Typical 13/ atypical 4 ^a

MP, maculopapular; EM, erythema multiforme; SJS, Stevens–Johnson syndrome; TEN, toxic epidermal necrolysis; DIHS, drug-induced hypersensitivity syndrome; DRESS, drug reaction with eosinophilia and systemic symptoms. ^aTypical, with reactivation of human herpesvirus (HHV)-6; atypical, without reactivation of HHV-6.

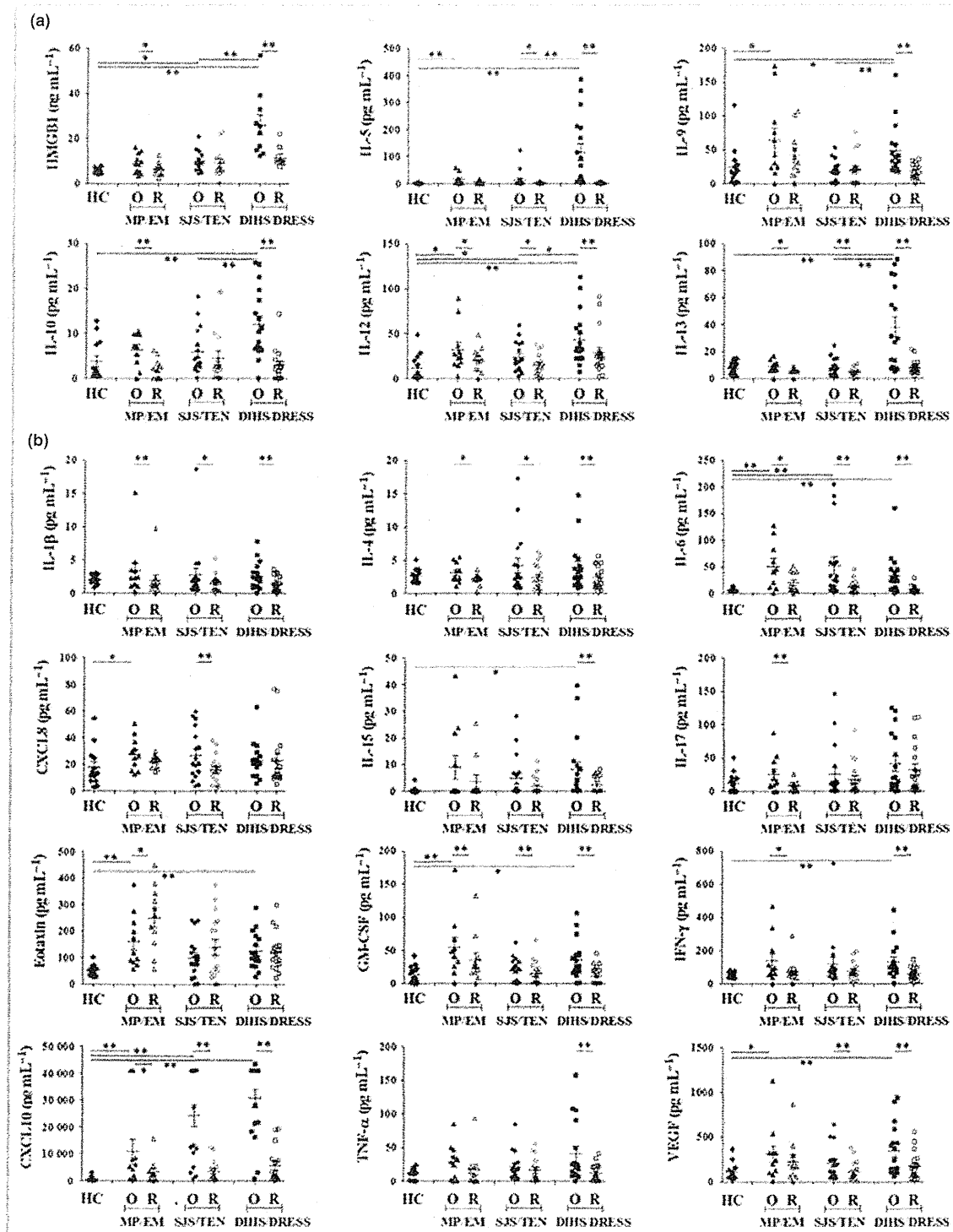


Fig 1. Serum high mobility group box 1 protein (HMGB1) and cytokine levels were analysed by enzyme-linked immunosorbent assay and luminometric bead array. To compare cytokine levels between healthy controls (HC) and each cutaneous adverse drug reaction (cADR) group at onset and between onset and recovery in each cADR group, the Mann-Whitney test and Wilcoxon matched-pairs tests were used, respectively. Significantly higher levels of (a) cytokines and (b) other proinflammatory cytokines in drug-induced hypersensitivity syndrome (DIHS)/drug reaction with eosinophilia and systemic symptoms (DRESS) than in Stevens-Johnson syndrome (SJS)/toxic epidermal necrolysis (TEN). CXCL, chemokine (C-X-C) motif ligand; EM, erythema multiforme; GM-CSF, granulocyte macrophage colony-stimulating factor; IFN, interferon; IL, interleukin; MP, maculopapular; O, onset of disease; R, recovery from disease; TNF, tumour necrosis factor; VEGF, vascular endothelial growth factor. **P* < 0.05. ***P* < 0.01.

during the acute stage of DIHS but not of TEN, whereas Tregs decrease dramatically in the late stage of DIHS.¹⁰ Taken together, HMGB1 released during the acute phase of DIHS/DRESS might facilitate Th2 cell activation induced by the causative drug, resulting in exacerbation. In this context, Th2 cells and Tregs, both producing IL-10, along with other activated cells producing proinflammatory cytokines, characterize the pathophysiology of DIHS/DRESS in the early stage.

In conclusion, cytokine storm occurs in various types of cADRs, but factors other than cytokines are required for the onset of severe cADR. HMGB1 may contribute to the development of DIHS/DRESS through Th2 cell activation, which plays a key role together with Tregs in the disease. The involvement of HMGB1 in cADRs therefore requires further investigation.

¹Department of Environmental Immunodermatology, Yokohama City University Graduate School of Medicine, Yokohama, Japan

²Department of Dermatology, Yokohama City University Medical Center, Yokohama, Japan

³National Epilepsy Center, Shizuoka Institute of Epilepsy and Neurological Disorders, Shizuoka, Japan

⁴Department of Dermatology, International University of Health and Welfare, Atami, Japan

E-mail: fuji_fuji_fuji_0101@yahoo.co.jp

H. FUJITA¹
S. MATSUKURA²
T. WATANABE¹
N. KOMITSU¹
Y. WATANABE¹
Y. TAKAHASHI³
T. KAMBARA²
Z. IKEZAWA⁴
M. AIHARA¹

activity in drug-induced hypersensitivity syndrome (DIHS)/drug rash with eosinophilia and systemic symptoms (DRESS). *J Dermatol Sci* 2013; **69**:38–43.

- 8 Liu QY, Yao YM, Yan YH et al. High mobility group box 1 protein suppresses T cell-mediated immunity via CD11c^{low}CD45RB^{high} dendritic cell differentiation. *Cytokine* 2011; **54**:205–11.
- 9 Hashizume H, Fujiyama T, Kanebayashi J et al. Skin recruitment of monomyeloid precursors involves human herpesvirus-6 reactivation in drug allergy. *Allergy* 2013; **68**:681–9.
- 10 Takahashi R, Kano Y, Yamazaki Y et al. Defective regulatory T cells in patients with severe drug eruptions: timing of the dysfunction is associated with the pathological phenotype and outcome. *J Immunol* 2009; **182**:8071–9.

Funding sources: This work was supported by a JSPS KAKENHI grant, number 24790534, and by Health and Labour Sciences Research grants (Research on Intractable Diseases) from the Ministry of Health, Labour and Welfare of Japan (H22-nanchi-ippan-003).

Conflicts of interest: none declared.

A case of pemphigus herpetiformis-like atypical pemphigus with IgG anti-desmocollin 3 antibodies

DOI: 10.1111/bjd.13088

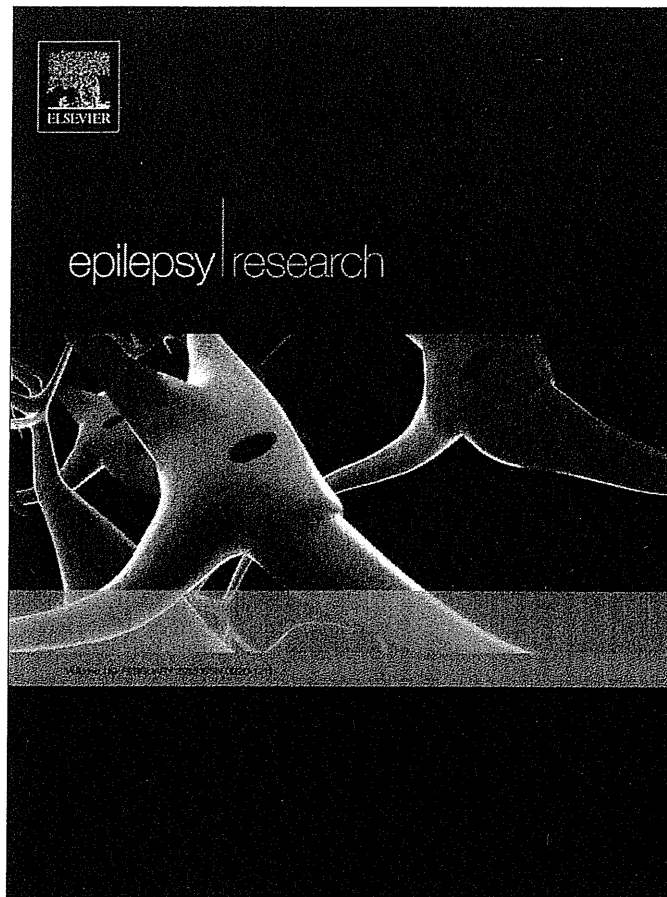
DEAR EDITOR, Pemphigus is an autoimmune blistering skin disease characterized by autoantibodies to keratinocyte cell surface antigens.¹ Major autoantigens for pemphigus are desmogleins (Dsgs), transmembrane cell–cell adhesion proteins belonging to the cadherin family. Dsg1 and Dsg3 are antigens for pemphigus foliaceus and pemphigus vulgaris, respectively. In addition to the four Dsg isoforms (Dsg1–4), there is another group of desmosomal cadherins, the desmocollins (Dsc), which is composed of three isoforms (Dsc1–3).

Pemphigus herpetiformis (PH) is a distinct variant of pemphigus; clinically it shows dermatitis herpetiformis-like features characterized by pruritic annular erythemas with vesicles on the periphery, histopathologically, eosinophilic spongiosis and immunologically, IgG antibodies to keratinocyte cell surfaces.² Ishii et al. reported that the targets of IgG autoantibodies in PH were Dsgs.³ Anti-Dsg1 antibodies were detected in the majority of patients, while anti-Dsg3 antibodies were detected in some cases. In this study, we report a case of PH-like atypical pemphigus with IgG antibodies to Dsc3, but without antibodies to Dsgs.

A 57-year-old Japanese man visited us complaining of a 1-year history of erosive skin lesions. He was otherwise healthy with no particular medical history. Physical examination revealed pruritic, urticarial, annular erythemas on the trunk and extremities, with some showing small vesicles at the periphery (Fig. 1a). No mucosal involvement of the oral cavity was present. Blood tests and computed tomography showed no abnormalities.

References

- 1 Shiohara T, Inaoka M, Kano Y. Drug-induced hypersensitivity syndrome (DIHS): a reaction induced by a complex interplay among herpesviruses and antiviral and antidrug immune responses. *Allergol Int* 2006; **55**:1–8.
- 2 Yoshikawa T, Fujita A, Yagami A et al. Human herpesvirus 6 reactivation and inflammatory cytokine production in patients with drug-induced hypersensitivity syndrome. *J Clin Virol* 2006; **37** (Suppl. 1):S92–6.
- 3 Chung WH, Hung SI. Recent advances in the genetics and immunology of Stevens–Johnson syndrome and toxic epidermal necrolysis. *J Dermatol Sci* 2012; **66**:190–6.
- 4 Harris HE, Andersson U, Pisetsky DS. HMGB1: a multifunctional alarmin driving autoimmune and inflammatory disease. *Nat Rev Rheumatol* 2012; **8**:195–202.
- 5 Nakajima S, Watanabe H, Tohyama M et al. High-mobility group box 1 protein (HMGB1) as a novel diagnostic tool for toxic epidermal necrolysis and Stevens–Johnson syndrome. *Arch Dermatol* 2011; **147**:1110–12.
- 6 Hirahara K, Kano Y, Mitsuyama Y et al. Differences in immunological alterations and underlying viral infections in two well-defined severe drug eruptions. *Clin Exp Dermatol* 2010; **35**:863–8.
- 7 Ogawa K, Morito H, Hasegawa A et al. Identification of thymus and activation-regulated chemokine (TARC/CCL17) as a potential marker for early indication of disease and prediction of disease



This article appeared in a journal published by Elsevier. The attached copy is furnished to the author for internal non-commercial research and education use, including for instruction at the authors institution and sharing with colleagues.

Other uses, including reproduction and distribution, or selling or licensing copies, or posting to personal, institutional or third party websites are prohibited.

In most cases authors are permitted to post their version of the article (e.g. in Word or Tex form) to their personal website or institutional repository. Authors requiring further information regarding Elsevier's archiving and manuscript policies are encouraged to visit:

<http://www.elsevier.com/authorsrights>



An analysis of epileptic negative myoclonus by magnetoencephalography



Masaki Yoshimura*, Shouwen Zhang, Yuki Ueda,
Kazumi Matsuda, Katsumi Imai, Yukitoshi Takahashi, Yushi Inoue

National Epilepsy Center, Shizuoka Institute of Epilepsy and Neurological Disorders, Urushiyama 886,
Aoi-ku 420-8688, Shizuoka, Japan

Received 8 June 2014; received in revised form 26 November 2014; accepted 3 December 2014
Available online 13 December 2014

KEYWORDS

Negative myoclonus;
Magnetoencephalography;
Cortical dysplasia;
Epilepsy;
Silent-periodlocked-averaging

Summary

Purpose: To clarify the neurophysiologic mechanism of epileptic negative myoclonus (ENM), we analyzed the magnetoencephalography (MEG) of a patient with ENM.

Methods: The 52-year-old right-handed male had frequent ENM in the right upper limb during awake and monthly seizures with sudden tonic stiffening of the right forearm during sleep. MRI demonstrated a focal cortical dysplasia in the cortex of the posterior portion of the left superior frontal sulcus. Whole-head type MEG, electroencephalography and electromyography were simultaneously recorded during ENM. Single equivalent currents dipoles (ECDs) were calculated for each spike component followed by silent period (SP) in the right deltoid muscle. These MEG spike components were averaged with respect to their peaks, and single ECD was also calculated for the averaged spike component. Furthermore, we analyzed the MEG with the silent-period-locked-averaging (SPLA) method. Twenty MEG signal data were averaged with respect to the onset of SP. Twenty epochs in each of five separate periods of recording were repeatedly averaged. ECDs were calculated for spike components observed in each averaged epoch.

Results: ECDs of each spike followed by SP were clustered near the cortex of the left central sulcus. In MEG spike averaging and SPLA method, ECDs at the peak of spike components were located near the right shoulder division of the primary sensorimotor cortex reproducibly. ECDs on the ascending phase before the peak were located lateral to the above ECD location in MEG spike averaging method.

* Corresponding author. Tel.: +81 54 245 5446; fax: +81 54 247 9781.

E-mail addresses: yosimura@szec.hosp.go.jp (M. Yoshimura), george12188@126.com (S. Zhang), ueda.de.yulgi@gmail.com (Y. Ueda), matsuda-1@hosp.go.jp (K. Matsuda), imaik-1@hosp.go.jp (K. Imai), takahashi-ped@umin.ac.jp (Y. Takahashi), yinoue-jes@umin.net (Y. Inoue).

Conclusions: ENM was produced by an inhibitory action on the primary sensorimotor cortex corresponding to the body segment in which ENM occurs.
© 2014 Elsevier B.V. All rights reserved.

Introduction

Epileptic negative myoclonus (ENM) is defined as an interruption of tonic muscle activity, which is time-locked to an epileptic electroencephalography (EEG) abnormality, without evidence of an antecedent positive myoclonus (Tassinari et al., 1995). This EEG abnormality is usually a spike over the contralateral central region, and is accompanied by a silent electromyography (EMG) period (SP) lasting for approximate 100 to 400 (less than 500) ms (Tassinari, 1981).

Although there have been some reports indicating particular cortical areas associated with ENM, the neurophysiological mechanisms for the genesis of ENM remain incompletely understood. Some of these reports indicate that ENM is produced by an inhibitory action on the primary sensorimotor region in non-invasive (Guerrini et al., 1993; Oguni et al., 1998; Capovilla et al., 2000; Kubota et al., 2005; Song et al., 2006; Yu et al., 2009) and invasive studies such as subdural electroencephalography (EEG) (Noachtar et al., 1997) and cortical electrical stimulation (Ikeda et al., 2000). On the other hand, some authors emphasize the involvement of the premotor cortex including the supplementary motor area in the generation of ENM by non-invasive procedures (Rubboli et al., 1995; Baumgartner et al., 1996; Meletti et al., 2000; Usui et al., 2010) and by cortical electrical stimulation (Rubboli et al., 2006). In non-invasive studies, change of regional blood flow, regional amount of benzodiazepine receptors or change of regional glucose uptake were demonstrated in association with ENM. Electrophysiological events such as epileptic discharges may reflect the generation of ENM directly. Compared to scalp EEG, Magnetoencephalography (MEG) can more accurately localize the sources of intraneuronal electric currents. There were only few reports on MEG analysis of ENM (Kubota et al., 2005). We here report the ictal MEG analysis in a case with ENM.

Methods

Patient

The patient was a 52-year-old right-handed male with two types of seizures. The first type of seizure was characterized by a sudden tonic stiffening with an extension of the right upper arm, often followed by a brief clonic convulsion in the right forearm. The total duration did not exceed 20 s and consciousness was always preserved during the seizure. Seizures occurred 1 to 4 times a month only during sleep, except for the first seizure at the age of 9 years. He started taking phenytoin and phenobarbital at 14 years of age. At around 39 years of age, ENM, the second seizure type, began noticed during waking period everyday. ENM was characterized by short repetitive loss of postural tone of the right upper extremity occurring ten to twenty times per

minute when the arms were held outstretched. Consciousness was fully preserved during the episodes of ENM.

Neurological examination showed no weakness, sensory deficit, nor cerebellar signs. 1.5-Tesla MR FLAIR, T1-, and T2-weighted images of the brain showed a high intensity lesion regarded as focal cortical dysplasia, located in the cortex of the posterior portion of the left superior frontal sulcus (Fig. 1).

EEG recorded with the international 10–20 system (EEG-1100, Nihon Kohden, Japan) showed frequent interictal focal spikes at electrodes C3, P3 and Cz without change of EMG in sleep and resting (Fig. 2). On the other hand, SPs of 80–200 ms duration (ENM) in the right deltoid muscle were seen in synchronization with spikes in the same area when the patient held his arms outstretched (Fig. 3a).

In seizures with tonic stiffening of the right upper arm, EEG showed fast activity with a maximum amplitude at electrodes C3 and Cz accompanied with attenuation of the interictal spikes a few seconds before the seizure onset, with a gradual increase in amplitude and a gradual decrease in frequency, disappearing 10–15 s after the seizure onset (Fig. 2).

Simultaneous MEG, EEG and EMG recording

MEG, EEG and EMG were simultaneously recorded in a magnetically shielded room. The neuromagnetic fields were recorded with a 160-channel whole head type axial gradiometer MEG system (PQ1160C; Yokogawa Electric Corporation, Japan). EEG was recorded with silver–silver chloride cap electrodes the international 10–20 system. EEG was recorded with 21 silver–silver chloride cap electrodes positioned in accordance with the international 10–20 system. Surface EMG electrodes were placed on the right deltoid muscle. The recording passband was 4–100 Hz in MEG and 1–100 Hz in EEG and 50–100 Hz in EMG, and the sampling rate was 500 Hz. For the purpose of reduce the influence of low frequency components of background activity, 4 Hz high-pass filter was used in MEG. During the recording of 6 min, the patient lay down and was asked to hold his right upper limb extended obliquely upward 30 degrees from the horizontal plane to induce ENMs.

Estimate of equivalent currents dipoles (ECDs) for each spike

We calculated single equivalent currents dipoles (ECDs) for each spike component followed by SP of 80–500 ms duration in the right deltoid muscle observed during the recording, using an iterative least squares minimization algorithm (Hämäläinen et al., 1993). ECDs with a goodness of fit (GOF) higher than 80% were accepted and overlaid onto MRI with five adhesive marker coils attached to the skin of the subject's head (10 mm in front of the left and the right tragus,

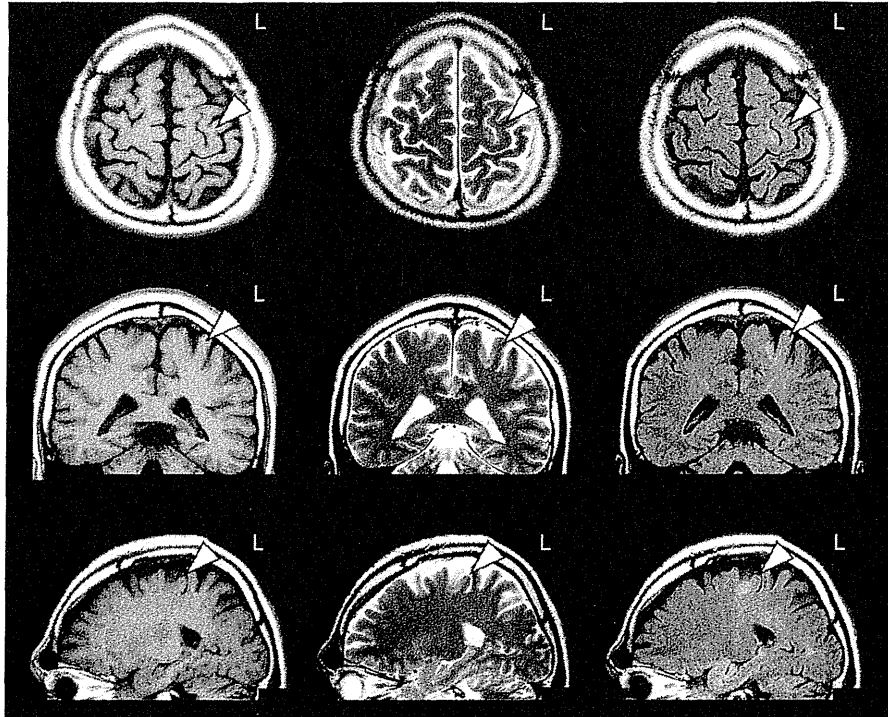


Fig. 1 1.5-T MRI of the brain. FLAIR, T1-, and T2-weighted images showed a high intensity lesion, regarded as focal cortical dysplasia, located in the cortex of the posterior portion of the left superior frontal sulcus.

35 mm above the nasion, and 40 mm right and left of that), by which the position of the subject's head relative to the MEG instrument was determined. Multiplanar head 3D-MRI was obtained by a 1.5 T MRI System (Signa Twin Speed 1.5 T system; Yokogawa Electric Corporation, Japan).

MEG spike averaging

For the purpose of minimizing the error from background activity, we averaged off-line 45 MEG spike components followed by SP of 80–500 ms duration in the right deltoid

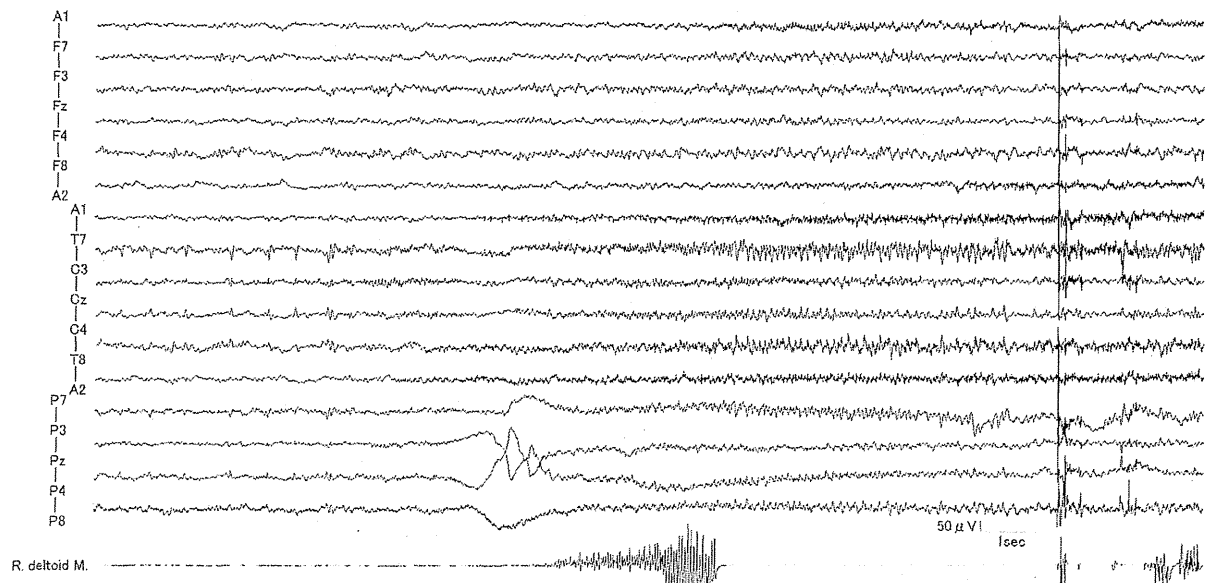


Fig. 2 A seizure with tonic stiffening of the right upper arm recorded during sleep. During interictal periods, EEG showed frequent focal spikes at electrodes C3, P3 and Cz without change of EMG. A few seconds before the onset of a seizure, the interictal spikes disappeared and fast activity maximum at electrodes C3 and Cz appeared and gradually increased the amplitude.

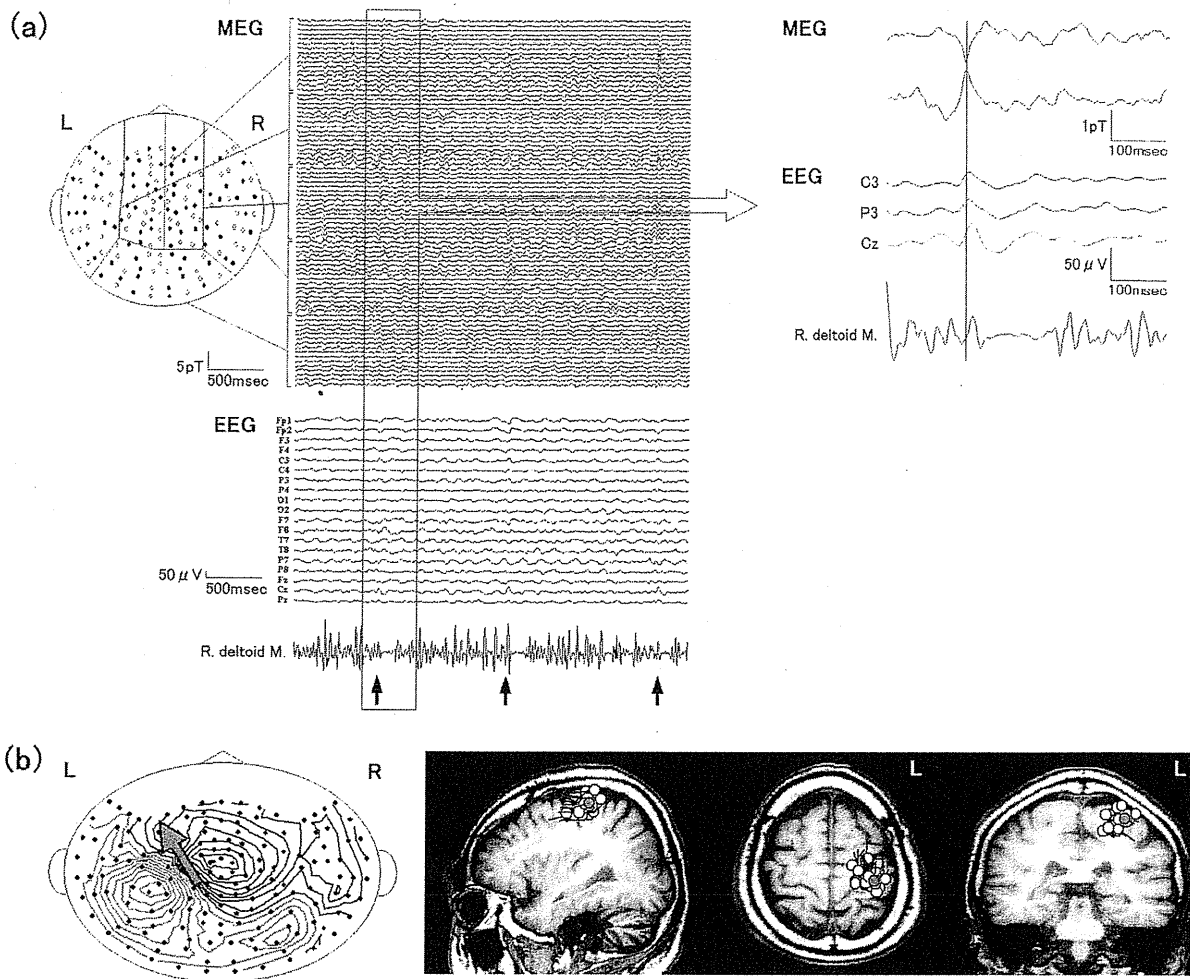


Fig. 3 Simultaneous records of MEG, EEG and EMG of the right deltoid muscle while the patient held outstretched his arms. (a) Paroxysms on MEG were observed as monophasic spikes in synchronization with focal spikes at electrodes C3, P3 and Cz on EEG which preceded silent periods in the right deltoid muscle. (b) The magnetic fields of peaks of each spike showed clear single dipole pattern, and equivalent currents dipoles of accepted 25 spikes were clustered near the cortex of the left central sulcus.

muscle aligned to their peaks (Wennberg and Cheyne, 2014). ECD was calculated for the averaged spike component and overlaid onto MRI.

Silent-period-locked-averaging

For the purpose of clarifying the spatiotemporal correlation between the ENM and generator sources of spikes, we analyzed the MEG with the silent-period-locked-averaging (SPLA) method (Ugawa et al., 1989). The MEG signal data was averaged off-line with respect to the onset of SP determined visually in the EMG of the right deltoid muscle. Twenty consecutive epochs starting 200 ms before and terminating 300 ms after each onset of SP were averaged. For confirming the reproducibility, twenty epochs in each of five separate periods of recording were repeatedly averaged. ECDs were calculated for spike components observed in each averaged

epoch and those with a GOF higher than 80% were overlaid onto MRI.

Somatosensory evoked fields (SEFs) to median nerve stimulation

For localizing the central sulcus and confirming the spatial relation with the sources of spikes, somatosensory evoked fields (SEFs) were measured with the same system in an awake state. The right median nerve was stimulated at the wrist with a constant-current pulse of 0.2 ms duration at a strength of 8.0 mA, three times above the sensation threshold. The analysis time was 50 ms before and 200 ms after the stimuli. The results of 500 trials were averaged, and ECD of the component of the SEF correspond to N20 in somatosensory evoked potentials was calculated and overlaid onto MRI.

Written informed consent was obtained from the patient.

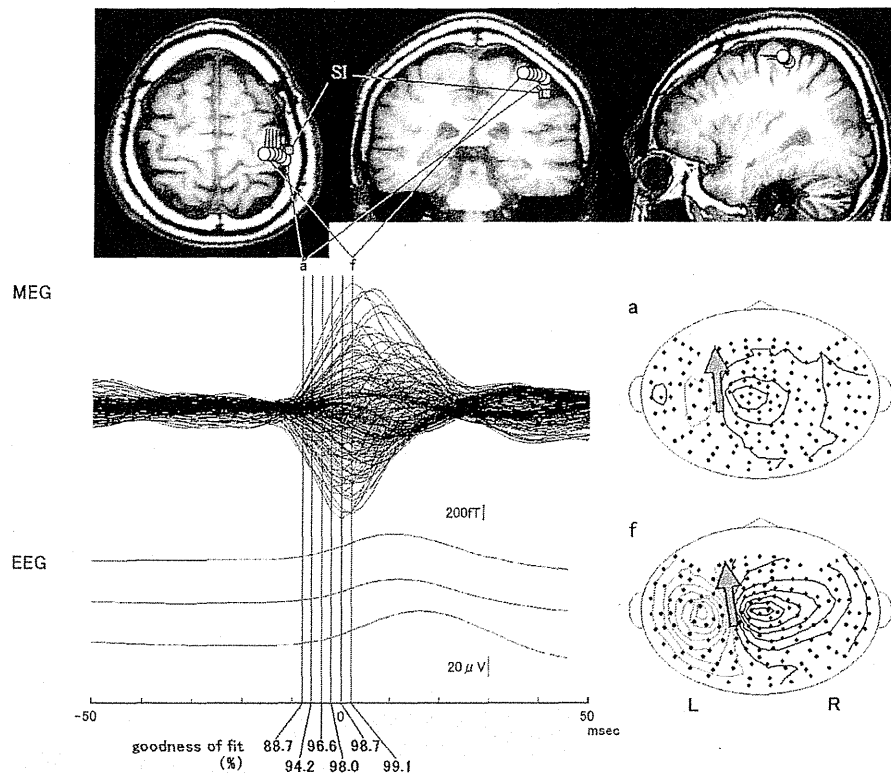


Fig. 4 MEG spike component averaged with respect to each peak of 45 MEG spike components, and the location of the equivalent currents dipoles (ECDs) of the peak and the ascending phase before the peak. ECD of the peak of the averaged MEG spike component was located on the precentral cortex about 18mm medial to the primary hand sensory cortex obtained by SEF study. ECDs on the ascending phase before the peak were located lateral to the above ECD location. SI: the primary hand sensory cortex.

Results

Estimate of ECDs for each spike

Paroxysms on MEG were observed as monophasic spikes in synchronization with focal spikes at electrodes C3, P3 and Cz on EEG which preceded SPs in the right deltoid muscle (Fig. 3a). Twenty-five spike components were accepted. The magnetic fields of peaks of each spike showed a clear single dipole pattern and ECDs were clustered near the cortex of the left central sulcus (Fig. 3b).

MEG spike averaging

ECD of the peak of the averaged MEG spike component was located on the precentral cortex with 99.1% of GOF. The obtained source was located in the area about 18 mm medial to the primary hand sensory cortex obtained by SEF study. ECDs on the ascending phase before the peak were located lateral to the above ECD location with 88.7 to 98.7% of GOF (Fig. 4).

SPLA

Five averaged waveforms of SPLA showed monophasic spikes on MEG with each peak at 40-46 ms before the onset of SPs

in the EMG of the right deltoid muscle. Since the MEG spikes preceded the spikes on EEG by about 12 ms, the latency between the peak of the EEG spikes and the onset of SPs was about 30 ms. ECD of each peak of MEG spikes was located on the precentral cortex reproducibly. The obtained sources were located in the area about 18 mm medial to the primary hand sensory cortex obtained by SEF study (Fig. 5).

Discussion

Though MEG is regarded as useful for locating a source of epileptic discharges with high spatial resolution, the method of analyzing a single ECD has some problems, including the error from background activity. Therefore, we analyzed the MEG with the MEG spike averaging and SPLA method in this report. MEG spike averaging is expected to minimize the error from background activity. However, some of spikes could be also related to ENM in extra-deltoid muscles in the right upper extremity, and spikes located in different areas could be averaged with the spike averaging method. On the other hand, it is considered that the SPLA method minimalizes the effect of changes in magnetic field except those generating ENM in the target muscle. In the present study, the current source of spikes from the MEG analysis with the SPLA method was reproducibly located on the precentral cortex about 18 mm medial to the primary

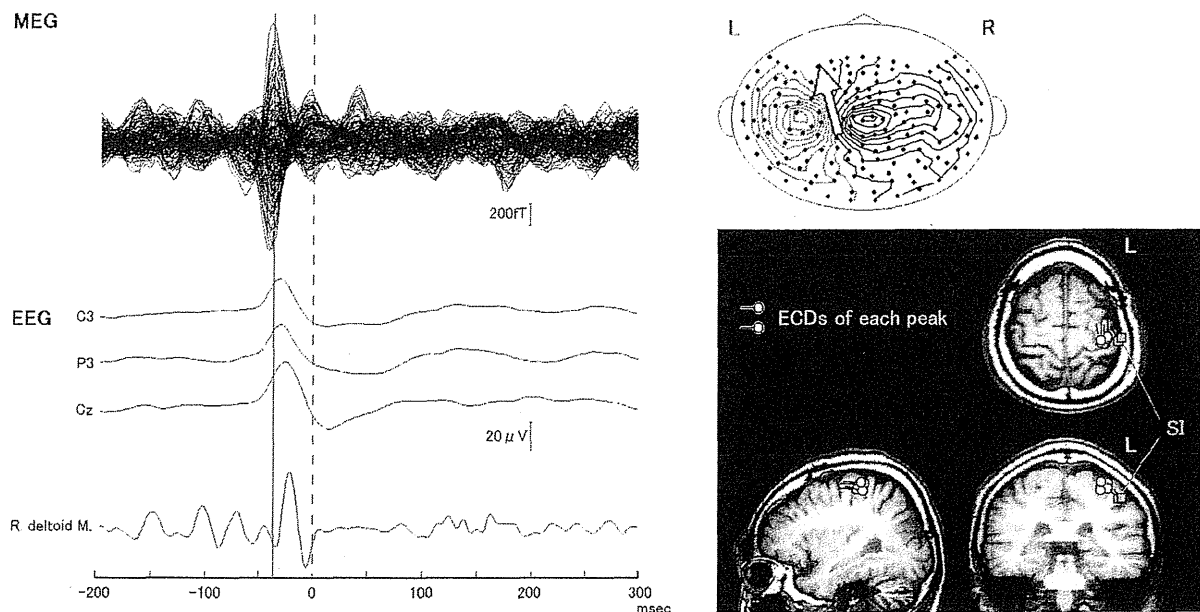


Fig. 5 Silent-period-locked-averaging (SPLA) MEG and EEG, and equivalent currents dipole (ECD) locations of each peak of five SPLA MEG. Averaged waveforms of SPLA showed monophasic spikes on MEG with each peak at 40–46 ms before the onset of silent periods in the EMG of the right deltoid muscle. ECDs of each peak of MEG spikes were reproducibly located on the precentral cortex about 18 mm medial to the primary hand sensory cortex obtained by SEF study. SI: the primary hand sensory cortex.

hand sensory cortex. This location was considered as near the right shoulder division of the primary motor cortex. Although same result was obtained with the spike averaging method, ECDs on the ascending phase before the peak were located lateral to the above location. It indicates that the main current source of spikes associated with ENM in the right deltoid muscle was located near the right shoulder division of the primary motor cortex, and probably propagates from the cortex lateral to it.

The characteristics of ENM in our cases were consistent with previous studies. The SPs duration of 80–200 ms and the latency of about 30 ms between the peak of the spikes and the onset of SPs observed in our case were in agreement with the findings of the others, in which the latency was reported as 20–40 ms (Guerrini et al., 1993; Baumgartner et al., 1996; Noachtar et al., 1997; Capovilla et al., 2000; Meletti et al., 2000; Usui et al., 2010) except for 50 ms in a case of Oguni et al. (1998). Some authors have reported cases with ENM and associated EEG transients in the contralateral primary sensorimotor cortex (Guerrini et al., 1993; Noachtar et al., 1997; Oguni et al., 1998; Capovilla et al., 2000; Kubota et al., 2005; Song et al., 2006). Furthermore a correlation between the occurrence of ENM in a body segment and a somatotopic topography on the scalp of the related paroxysmal activity has been suggested. For example ENM in an upper limb was associated with an EEG transient in the contralateral central region (Guerrini et al., 1993), and ENM in a lower limb was suggested to be associated with a spike in the vertex area (Capovilla et al., 2000). In addition, Kubota et al. (2005) demonstrated by the MEG analysis that ENM of the bilateral hands or neck was associated with a spike of which the current source was localized mainly in the lower

precentral area including the neck and orofacial division of the primary motor cortex. They suggested from the beneficial effect of ethosuximide (a T-type Ca^{2+} channel blocker in thalamic neurons and the cortex) for ENM and the MEG results that an abnormal interaction of the thalamocortical network might be closely related to the pathogenesis of ENM. Our result is in agreement with these studies in that the current source of spikes associated with ENM by the MEG analysis was estimated in the precentral cortex corresponding to the body segment in which ENM occurs, and indicates that ENM is produced by an inhibitory action on the primary sensorimotor region. This is corroborated by the finding of the cortical electrical stimulation, in which Ikeda et al. (2000) have demonstrated that the inhibitory mechanism within the primary sensorimotor area, but not in the non-primary motor areas, plays an important role in eliciting negative myoclonus because single pulse stimulation of primary sensorimotor area exclusively elicited a SP.

On the other hand, some studies have indicated the involvement of the premotor cortex including a supplementary motor area in the generation of ENM (Rubboli et al., 1995, 2006; Baumgartner et al., 1996; Meletti et al., 2000; Usui et al., 2010). Usui et al. (2010) reported a case with a deficit in GABA-A receptors in the supplementary motor area by ^{123}I IMZ-SPECT image, and a case reported by Meletti et al. (2000) had ENM and asymmetric tonic seizures regarded as having a supplementary sensorimotor area origin. These findings suggest the presence of functional abnormality in supplementary motor area in patients with ENM. Tassinari et al. (1995) demonstrated that the focal spike associated with ENM was involving, primarily or secondarily, the centroparietal and frontal supplementary motor areas, and that

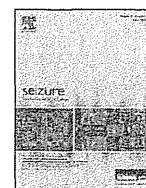
a cortical inhibitory active mechanism plays an important role in the genesis of ENM. In our case, unlike the cases in these reports, ENM did not originate in the supplementary motor area, although the premotor cortex may be functionally involved in the genesis of ENM.

Conclusion

In our case, MEG analysis with the SPLA method and with the spike averaging method showed that ENM was produced by an inhibitory action on the primary sensorimotor cortex corresponding to the body segment in which ENM occurs.

References

- Baumgartner, C., Podreka, I., Olbrich, A., Novak, K., Serles, W., Aull, S., Almer, G., Lurger, S., Pietrzyk, U., Prayer, D., Lindinger, G., 1996. Epileptic negative myoclonus: an EEG-single-photon emission CT study indicating involvement of premotor cortex. *Neurology* 46, 753–758.
- Capovilla, G., Rubboli, G., Beccaria, F., Meregalli, S., Veggiotti, P., Giambelli, P.M., Meletti, S., Tassinari, C.A., 2000. Intermittent falls and fecal incontinence as a manifestation of epileptic negative myoclonus in idiopathic partial epilepsy of childhood. *Neuropediatrics* 31, 273–275.
- Guerrini, R., Dravet, C., Genton, P., Bureau, M., Roger, J., Rubboli, G., Tassinari, C.A., 1993. Epileptic negative myoclonus. *Neurology* 43, 1078–1083.
- Hämäläinen, M., Hari, R., Ilmoniemi, R., Knuutila, J., Lounasmaa, O.V., 1993. Magnetoencephalography—theory, instrumentation, and applications to noninvasive studies of signal processing in the human brain. *Rev. Mod. Phys.* 65, 413–497.
- Ikeda, A., Ohara, S., Matsumoto, R., Kunieda, T., Nagamine, T., Miyamoto, S., Kohara, N., Taki, W., Hashimoto, N., Shibasaki, H., 2000. Role of primary sensorimotor cortices in generating inhibitory motor response in humans. *Brain* 123, 1710–1721.
- Kubota, M., Nakura, M., Hirose, H., Kimura, I., Sakakihara, Y., 2005. A magnetoencephalographic study of negative myoclonus in a patient with atypical benign partial epilepsy. *Seizure* 14, 28–32.
- Meletti, S., Tinuper, P., Bisulli, F., Santucci, M., 2000. Epileptic negative myoclonus and brief asymmetric tonic seizures. A supplementary sensorimotor area involvement for both negative and positive motor phenomena. *Epilept. Disord.* 2, 163–167.
- Noachtar, S., Holthausen, H., Lüders, H.O., 1997. Epileptic negative myoclonus: subdural EEG recordings indicate a postcentral generator. *Neurology* 49, 1534–1537.
- Oguni, H., Uehara, T., Tanaka, T., Sunahara, M., Hara, M., Osawa, M., 1998. Dramatic effect of ethosuximide on epileptic negative myoclonus: implications for the neurophysiological mechanism. *Neuropediatrics* 29, 29–34.
- Rubboli, G., Parmeggiani, L., Tassinari, C.A., 1995. Frontal inhibitory spike component associated with epileptic negative myoclonus. *Electroencephalogr. Clin. Neurophysiol.* 95, 201–205.
- Rubboli, G., Mai, R., Meletti, S., Francione, S., Cardinale, F., Tassi, L., Russo, G.L., Stanzani-Maserati, M., Cantalupo, G., Tassinari, C.A., 2006. Negative myoclonus induced by cortical electrical stimulation in epileptic patients. *Brain* 129, 65–81.
- Song, I.U., Lee, D.G., Kim, J.S., An, J.Y., Lee, S.B., Kim, Y.I., Lee, K.S., 2006. Unilateral epileptic negative myoclonus following focal lesion of the postcentral cerebral cortex due to acute middle cerebral infarction. *J. Clin. Neurool.* 2, 272–275.
- Tassinari, C.A., 1981. New perspectives in epileptology. In: *Proceedings of the International Public Seminar on Epileptology*, Tokyo, pp. 42–59.
- Tassinari, C.A., Rubboli, G., Parmeggiani, L., et al., 1995. Epileptic negative myoclonus. In: Fahn, S., Hallett, M., Lüders, H.O., Marsden, C.D. (Eds.), *Negative Motor Phenomena. Advances in Neurology*, vol. 67. Lippincott-Raven Publishers, Philadelphia, pp. 181–197.
- Ugawa, Y., Shimpo, T., Mannen, T., 1989. Physiological analysis of asterixis: silent period locked averaging. *J. Neurol. Neurosurg. Psychiatry* 52, 89–92.
- Usui, K., Matsuda, K., Terada, K., Nikaido, K., Matsushashi, M., Nakamura, F., Umeoka, S., Usui, N., Tottori, T., Baba, K., Inoue, Y., 2010. Epileptic negative myoclonus: a combined study of EEG and [¹²³I]iomazenil (¹²³I-IMZ) single photon emission computed tomography indicating involvement of medial frontal area. *Epilepsy Res.* 89, 220–226.
- Wennberg, R., Cheyne, D., 2014. Reliability of MEG source imaging of anterior temporal spikes: analysis of an intracranially characterized spike focus. *Clin. Neurophysiol.* 125, 903–918.
- Yu, H.Y., Kwan, S.Y., Lirng, J.F., Liao, K.K., Chu, Y.K., Liao, S.Q., 2009. Epileptic negative myoclonus: SPECT, PET, and video/EEG studies and the dramatic effects of levetiracetam. *Epilepsy Behav.* 14, 687–690.



Immediate suppression of seizure clusters by corticosteroids in PCDH19 female epilepsy



Norimichi Higurashi^{a,b}, Yukitoshi Takahashi^c, Ayako Kashimada^d, Yuji Sugawara^d, Hiroshi Sakuma^e, Yuko Tomonoh^f, Takahito Inoue^f, Megumi Hoshina^g, Ruri Satomi^h, Masaharu Ohfuⁱ, Kazuya Itomi^j, Kyoko Takano^k, Tomoko Kirino^l, Shinichi Hirose^{b,f,*}

^a Department of Pediatrics, Jikei University School of Medicine, 3-25-8, Nishi-Shimbashi, Minato-ku, Tokyo 105-8461, Japan

^b Central Research Institute for the Pathomechanisms of Epilepsy, Fukuoka University, 7-45-1, Nanakuma, Jonan-ku, Fukuoka 814-0180, Japan

^c National Epilepsy Center, Shizuoka Institute of Epilepsy and Neurological Disorders, Urushiyama 886, Aoi-ku, Shizuoka 420-8688, Japan

^d Department of Pediatrics, Tokyo Medical and Dental University, 1-5-45, Yushima, Bunkyo-ku, Tokyo 113-8510, Japan

^e Department of Brain Development and Neural Regeneration, Tokyo Metropolitan Institute of Medical Science, 2-1-6, Kamikitazawa, Setagaya-ku, Tokyo 156-8506, Japan

^f Department of Pediatrics, Fukuoka University School of Medicine, 7-45-1, Nanakuma, Jonan-ku, Fukuoka 814-0180, Japan

^g Department of Pediatrics, Ohara General Hospital, 6-11, Omachi, Fukushima 960-8611, Japan

^h Department of Pediatrics, JA Toride Medical Center, 2-1-1, Hongo, Toride, Ibaraki 302-0022, Japan

ⁱ Division of Child Neurology, Okinawa Prefectural Southern Medical Center & Children's Medical Center, 118-1, Aza Arakawa, Haebaru-cho, Shimajiri-gun, Okinawa 901-1193, Japan

^j Division of Neurology, Aichi Children's Health and Medical Center, 1-2, Osakada Morioka-cho, Obu, Aichi 474-8710, Japan

^k Department of Medical Genetics, Shinshu University School of Medicine, 3-1-1, Asahi, Matsumoto, Nagano 390-8621, Japan

^l Department of Pediatrics, Shikoku Medical Center for Children and Adults, 2-1-1, Senyu-cho, Zentsuji, Kagawa 765-8507, Japan

ARTICLE INFO

Article history:

Received 4 November 2014

Received in revised form 2 February 2015

Accepted 5 February 2015

Keywords:

Blood–brain barrier

Epilepsy and mental retardation limited to females (EFMR)

Inflammation

Neuronal antibody

N-methyl-D-aspartate (NMDA)-type

glutamate receptor

ABSTRACT

Purpose: The pathomechanism and treatment of PCDH19 female epilepsy (PCDH19-FE) remain unclear. Here, we report that corticosteroids are effective for control of the seizure clusters or other acute symptoms of PCDH19-FE and argue for the possible involvement of a compromised blood–brain barrier (BBB) in its pathogenesis.

Methods: The efficacy of corticosteroids was retrospectively reviewed in five Japanese patients with PCDH19-FE. The results of antibody assays against the N-methyl-D-aspartate-type glutamate receptor (abs-NR) in serum/cerebrospinal fluid were also compiled.

Results: Corticosteroid treatments significantly improved the acute symptoms, including seizure clusters, in all cases, most often immediately after the initial administration. However, the effect was transient, and some seizures recurred within a few weeks, especially in association with fever. Serum and/or cerebrospinal fluid abs-NR were detected in all patients. Target sequences of the detected antibodies were multiple, and the titers tended to decrease over time. In one patient, immunohistochemical analysis using rat hippocampal slices also revealed serum antibodies targeting an unknown epitope in neuronal cytoplasm.

Conclusion: Our findings imply an involvement of inflammatory processes in the pathogenesis of PCDH19-FE and therapeutic utility for corticosteroids as an adjunctive option in acute treatment. PCDH19 is well expressed in brain microvascular endothelial cells and thus its impairment may cause BBB vulnerability, which may be ameliorated by corticosteroids. The abs-NR detected in our patients may not indicate an autoimmune pathomechanism, but may rather represent non-specific sensitization to degraded neuronal components entering the general circulation, the latter process facilitated by the BBB vulnerability.

© 2015 British Epilepsy Association. Published by Elsevier Ltd. All rights reserved.

* Corresponding author at: Department of Pediatrics, School of Medicine, Fukuoka University, 45-1, 7-chome, Nanakuma, Jonan-ku, Fukuoka 814-0180, Japan.

Tel.: +81 92 801 1011; fax: +81 92 862 1290.

E-mail address: hirose@fukuoka-u.ac.jp (S. Hirose).

<http://dx.doi.org/10.1016/j.seizure.2015.02.006>

1059-1311/© 2015 British Epilepsy Association. Published by Elsevier Ltd. All rights reserved.

1. Introduction

A heterozygous defect in the gene encoding protocadherin 19 (*PCDH19*) causes early-onset intractable epilepsy in females (*i.e.*, *PCDH19*-related female epilepsy, *PCDH19*-FE, or previously, epilepsy and mental retardation limited to females, EFMR) [1]. *PCDH19*, an adhesion molecule of the δ 2-protocadherin subclass of the cadherin superfamily, is highly expressed in the vertebrate brain. δ -Protocadherins are intimately involved in brain development and neural functions, as well as in many neurological diseases [2]. However, the homophilic adhesion capacity of *PCDH19* by itself is low, and its exact function remains unclear.

The hallmark clinical feature of *PCDH19*-FE is recurrent seizure clusters consisting of brief focal seizures and/or generalized convulsions, which can be triggered by febrile or afebrile illnesses [3]. The seizures do not recur regularly, but once they recur, the cluster continues for days to weeks despite multiple treatments. Conventional antiepileptic drugs fail to control or prevent most of these seizures. Ictal symptoms and EEG findings indicate that the seizures mainly involve the limbic system and medial frontal region [4].

The clinical features indicate a possible immune/inflammation involvement in seizure generation, which could be a non-genetic modifier of the disease phenotype. In agreement with this, we have previously reported patients showing excellent efficacy of corticosteroids for seizure clusters [5]. We have also encountered cases having antibodies to the *N*-methyl-D-aspartate (NMDA)-type glutamate receptor (abs-NR) in the serum or cerebrospinal fluid (CSF). Abs-NR cause limbic encephalitis, predominantly in young women (anti-NMDA receptor encephalitis) [6], but may also appear secondarily and non-specifically in various neurologic diseases including epilepsy [7]. In the latter case, abs-NR are not significantly involved in the disease pathogenesis.

This study aims to explore whether corticosteroids have an ability to improve the seizures in *PCDH19*-FE and if any immune mechanism is involved. We retrospectively reviewed and summarized the clinical results of corticosteroid treatments as well as the results of an assay for abs-NR in Japanese patients. The potential significance of these findings with regard to the pathomechanisms of this disorder is also discussed.

2. Methods

2.1. Patients

Japanese patients with *PCDH19*-FE who received corticosteroid treatments and/or underwent the abs-NR assay were retrospectively studied. They were genetically diagnosed at Fukuoka University⁵ and clinical details were collected from their doctors in charge. Since the patients were children, the doctors obtained written informed consent from the parents before the blood and/or CSF samples were drawn for genetic analysis of *PCDH19* and/or for assay for abs-NR. Genetic analysis of *PCDH19* was approved by the ethics committee of Fukuoka University. The abs-NR assay was approved by the National Epilepsy Center, Shizuoka Institute of Epilepsy and Neurological Disorders.

2.2. ab-NR assay

The abs-NR assay was performed at National Epilepsy Center, Shizuoka Institute of Epilepsy and Neurological Disorders. Experimental details have been described elsewhere [8]. Briefly, serum and CSF samples were examined by enzyme-linked immunosorbent assay (ELISA) or, in one patient, by immunoblot

analysis targeting GluN2B. The ELISA target peptides were the extracellular N-terminal (NT) and/or intracellular C-terminal (CT) regions of the GluN2B, GluN1, and GluD2 subunits (Supplementary Table 1). Titers were determined by comparing the optical densities of our patients with those of 35 patients with non-inflammatory focal epilepsy, who served as controls. The results were expressed as number of standard deviations of the controls (SD) from the mean of the controls and were considered positive when ≥ 2 SD.

2.3. Immunohistochemical analysis for anti-neuronal autoantibodies

In two patients, the presence of anti-neuronal autoantibodies was further examined immunohistochemically using rat hippocampal slices exposed to serum or CSF from the patients. Experimental details are described in Supplementary information.

3. Results

Five patients (Patients 1–5) received corticosteroid treatments mainly during the acute phase before and/or after the diagnosis of *PCDH19*-FE. Abs-NR were examined in these patients mostly before corticosteroid administration and in four other patients (Patients 6–9). These tests were performed because autoimmune or inflammatory processes were clinically suspected in the pathogenesis of the epilepsy, although none of these patients except Patient 4 showed pleocytosis or an elevation of CSF protein level. Outlines of Patients 1, 2, and 5–9 have been described previously [3,5].

3.1. Efficacy of corticosteroid treatments

Treatment details and results are summarized in Table 1. The details of the clinical courses are described in Supplementary information. Overall, corticosteroids dramatically improved acute neurological symptoms: ongoing seizure clusters in Patients 1–3 and 5, and an acute encephalopathic episode that developed after a seizure cluster in Patient 4, were controlled. In most cases, the improvement was achieved after the first administration. In the cases of seizure cluster, the initial administration was conducted well in advance of the expected time of spontaneous remission of the cluster. Furthermore, in Patient 3, corticosteroids were initiated on the second day of each cluster to confirm that the cluster continued for more than 1 day despite midazolam administration. Regarding drugs and dosages, four young patients (Patients 1–4) received an intravenous drip infusion of 10–30 mg/kg methylprednisolone once daily, for up to 3 days. Patient 5 received an intravenous infusion of 0.35 mg/kg prednisolone once or twice, depending on the cluster, followed by oral administration of prednisolone at 1 mg/(kg·day) at age 11. However, as observed in Patients 1, 3, and 5, the effect was fundamentally transient; seizure clusters often recurred within a few weeks, especially when fever appeared.

For Patient 4, methylprednisolone was used at age 1 for an encephalopathic episode with decline of consciousness and systemic weakness, which abruptly developed 3 days after the termination of a one-day seizure cluster. EEG showed an increase of δ -waves, but no ictal activity. Mild CSF pleocytosis (85 cells/ μ L) was identified a week before the episode. These symptoms completely disappeared immediately after the initial administration of methylprednisolone.

For Patient 1, corticosteroids were administered prophylactically after age 3, with 3 days of oral betamethasone or prednisolone administration at times of fever appearance. After starting this treatment, no or only mild recurrences (not requiring hospitalization) were observed, even during fever.

Table 1
Details and efficacy of corticosteroid therapy.

Pt no	<i>PCDH19</i> mutation	Age at onset (m)	Age at CS TX	CS	Route & dose	Target symptom	Simultaneous TX	Usual duration of Sz cluster	Result	Present intellect
1	p.L719*	13	2y4m	mPSL	IV, 30 mg/kg, 3d	Sz cluster	MDL CBZ CZP VPA LTG LEV	Days ~2 wk	Disappeared after 1st IV	Normal 5y1m
			2y10m	mPSL	IV, 30 mg/kg, 3d	Sz cluster			Disappeared after 1st IV	
			2y11m	mPSL	IV, 30 mg/kg, 3d	Sz cluster			Recurred in 2 wk w/fever ^a	
			3y0m	mPSL	IV, 10 mg/kg, 3d	Sz cluster			Disappeared after 1st IV	
			3y4m	BET	Oral, 0.01 mg/kg, 3d	Sz prevention			Recurred in 1wk w/fever	
			4y1m	PSL	Oral, 1–1.5 mg/kg, 3d	Sz prevention			Disappeared after 1st IV	
2	p.K120Rfs*3	10	10m	mPSL	IV, 30 mg/kg, 3d	Sz cluster	MDL PB ACV IVIG EDV	–	Disappeared after 1st IV	Moderate delay 3y
									Recurred in 1wk	
3	p.D417H p.D596Y	5	1y11m	mPSL	IV, 20 mg/kg, 2d	Sz cluster	MDL fPHT CLB LEV KBr DZP	Days ~2wk	Disappeared after 1st IV	Normal 2y8m
			2y1m	mPSL	IV, 20 mg/kg, 3d	Sz cluster			Disappeared after 1st IV	
			2y2m	mPSL	IV, 20 mg/kg, 2d	Sz cluster			Disappeared after 1st IV	
			2y5m	mPSL	IV, 10 mg/kg, 1d fol. by 20 mg/kg, 1d	Sz cluster			Disappeared after 2nd IV	
			2y7m	mPSL	IV, 20 mg/kg, 1d	Sz cluster			Disappeared after 1st IV	
			2y7m	mPSL	IV, 20 mg/kg, 2d	Sz cluster			Recurred in 9d w/flu	
4	p.D596G	6	1y0m	mPSL	IV, 30 mg/kg, 3d	Encephalopathic symptoms	CBZ fPHT LDC PB	1d	Disappeared after 1st IV	Hyperactive 1y6m
5	p.D45Gfs*43	8	11y5m	PSL	IV, 0.35 mg/kg x1 fol. by Oral, 1 mg/kg ^b	Sz cluster	KBr CZP	Half a day	Disappeared after 1st IV	Moderate delay 11y8m
			11y6m	PSL	IV, 0.35 mg/kg x1 fol. by Oral, 1 mg/kg	Sz cluster			Disappeared after 1st IV	
			11y6m	PSL	IV, 0.35 mg/kg x1 fol. by Oral, 1 mg/kg	Sz cluster			Recurred in 1wk w/fever	
			11y8m	PSL	IV, 0.35 mg/kg x2 fol. by Oral, 1 mg/kg	Sz cluster			Disappeared after 1st IV	
								Disappeared after 2nd IV		

^a Noted when seizures recurred within 3 weeks after corticosteroid administration.

^b In Patient 5, oral prednisolone was gradually tapered off. Pt no, Patient number; m, month(s); CS, corticosteroid; TX, treatment; Sz, seizure; y, year(s); mPSL, methylprednisolone; BET, betamethasone; PSL, prednisolone; IV, intravenous route; d, day(s); MDL, midazolam; CBZ, carbamazepine; CZP, clonazepam; VPA, valproic acid; LTG, lamotrigine; LEV, levetiracetam; wk, week(s); PB, phenobarbital; ACV, acyclovir; IVIG, intravenous immunoglobulin; EDV, edaravone; fol. by, followed by; fPHT, fosphenytoin; CLB, clobazam; KBr, potassium bromide; DZP, diazepam; LDC, lidocaine.

3.2. *ab*-NR and further anti-neuronal autoantibody assays

Eight of the nine patients who underwent the assay showed positivity to multiple epitopes in the serum or CSF (Patients 1–7 and 9, 88.9%, Table 2). The epitopes included GluN1-NT, which has been reported to be critical for the emergence of neuropsychiatric symptoms in anti-NMDA-receptor encephalitis [6]. Patients 1 and 2 had high CSF titers of antibodies during the acute phase (>10 SD). Patient 6 showed positivity in the CSF at onset and in serum half a year later. Patients 3, 5, and 9 underwent follow-up assays, and their titers were found to decrease over time. In Patient 5, immunohistochemical analysis during seizure recurrence at age 11, using serum drawn before prednisolone administration, revealed autoantibodies to the cytoplasm of hippocampal neurons, as demonstrated in hippocampal slices taken from rats

(Supplementary Fig. b). The assay failed to identify the epitope. These results suggest that following seizure clusters, an immune reaction occurs non-specifically to degraded neuronal proteins, including NMDA-type glutamate receptor, inside and subsequently outside the brain. Such reactions appear to be strong at early ages, but do not show a uniform pattern.

4. Discussion

This study revealed the therapeutic potency of corticosteroids for acute symptoms in *PCDH19*-FE. The rapid and efficient response was remarkable and might be a useful indicator for this disease. The cases of Patients 1 and 9 suggested that oral corticosteroids taken during interictal periods might exert some prophylactic effects, but further assessments are necessary to establish this.